Proc. 2nd Japan-China Joint Workshop on Positron Science
JJAP Conf. Proc. **2** (2014) 011101

Cu Precipitates in Hydrogen Ion Irradiated Fe–0.3%Cu Alloy Investigated by Positron Annihilation Spectroscopy

Shuoxue Jin[1], Xingzhong Cao[1,*], Peng Zhang[1], Eryang Lu[1], Liping Guo[2], RunSheng Yu[1], and Baoyi Wang[1,*]

[1]*Key Laboratory of Nuclear Radiation and Nuclear Energy Technology, Institute of High Energy Physics, Chinese Academy of Sciences, Beijing 100049, China*
[2]*Key Laboratory of Artificial Micro- and Nano-structures of Ministry of Education and School of Physics and Technology, Wuhan University, Wuhan 430072, China*

E-mail: caoxzh@ihep.ac.cn, wangboy@ihep.ac.cn

(Received March 17, 2014)

The formation of Cu precipitates in Fe–0.3%Cu binary model alloy after hydrogen ion irradiation at 400 °C was investigated by positron annihilation spectroscopy using a slow positron beam. In order to study the effect of elevated temperature on the Cu precipitates, annealing treatment at 400 °C in Fe–0.3%Cu alloy was also investigated. The *S*-parameters of specimens increased with increasing irradiation dose, especially in the damage peak region. H^+ implantation produced a large number of vacancy-type defects in Fe–0.3%Cu alloy. Compared to the unirradiated samples, the irradiated specimens show an overall major increase in the *W* parameter values. The experimental results indicate that Cu precipitates formed easily under a low irradiation dose at elevated temperature. No obvious Cu precipitates formed when unirradiated Fe–0.3%Cu alloy was annealed for 2 h at 400 °C.

1. Introduction

Irradiation-hardening, leading to an increase in the ductile-to-brittle transition temperature (DBTT), has been widely recognized in nuclear reactor pressure vessels (RPV) [1]. Cu atoms have a very low solubility in α-Fe [2, 3], thus, high-energy particle irradiation or thermal treatment at elevated temperature could lead the formation of Cu precipitates in FeCu alloys [4]. Cu precipitates are a major contributor to the increase in hardness and embrittlement, which results from the interaction of Cu with defects induced by irradiation. Previous studies have focused extensively on the formation of Cu precipitates in RPV steels irradiated by neutrons/ions [3, 5–9]. Yoshiie *et al*. reported the effect of the damage rate on Cu precipitation and indicated that precipitation was accelerated at a lower damage rate [10]. Nagai *et al*. have concluded that voids were surrounded by Cu precipitates [11]. Xu *et al*. also detected the formation of Cu cluster-vacancies complexes, and concluded that the growth of Cu precipitates depended on the nucleation and growth of microvoids, which did not increase monotonically with increasing irradiation dose [2, 4]. Cao *et al*. indicated that the precipitation of Cu atoms formed easily with low irradiation dose [5]. Therefore, it is important to establish a fundamental understanding of the interactions between Cu precipitates and the formation of vacancy-type defects. Hori *et al*. indicated that high density of vacancies introduced by heavy ions enhanced the formation of nm-size copper precipitates [12]. However, the mechanism of the interaction between defects and fine Cu-rich precipitates under irradiation remains unclear, further investigation is required, especially concerning the interaction between vacancies and copper atoms and the nucleation of Cu precipitates at low irradiation dose [2,5]. In order to clarify the effect of irradiation defects on the formation of Cu precipitates, it is important to study the fundamental behavior of the interaction between irradiation induced defects and Cu atoms. Ion implantation/irradiation is the most useful technique to introduce defects in metal materials [12] and hydrogen ions are considered to be the most suitable ion to sim-

ulate neutron irradiation [13]. In the present work, positron annihilation Doppler Broadening (DB) spectroscopy and Coincidence Doppler Broadening (CDB) methods were used to measure the defects and the Cu precipitation behavior in hydrogen ion irradiated Fe–0.3%Cu alloy.

2. Experimental procedure

2.1 Materials and preparation

The Fe–0.3%Cu model alloy used in the present study was melted from Fe (99.99 % purity) and Cu (99.9 % purity) in vacuum using a high-frequency induction furnace, where the composition of Cu is in wt%. After melting, solution treatment of the samples consisted of heating at 800 °C for 24 h, followed by quenching in ice water. The bulk materials were first cut to a thickness of 1 mm in 10 mm × 10 mm square sheets and then cold-rolled to a thickness of about 0.5 mm. All samples were then punched into 10 mm × 10 mm square sheets, well-annealed at 900 °C for 0.5 h in vacuum, and quenched in ice water. Before hydrogen ion irradiation, the samples were electrochemically polished to a mirror-like surface using 25 % perchloric acid and 75 % ethanol polishing solution at −30 °C. Finally, the polished sheet samples were cleaned with acetone and ultrasonically rinsed in de-ionized water for 5 min.

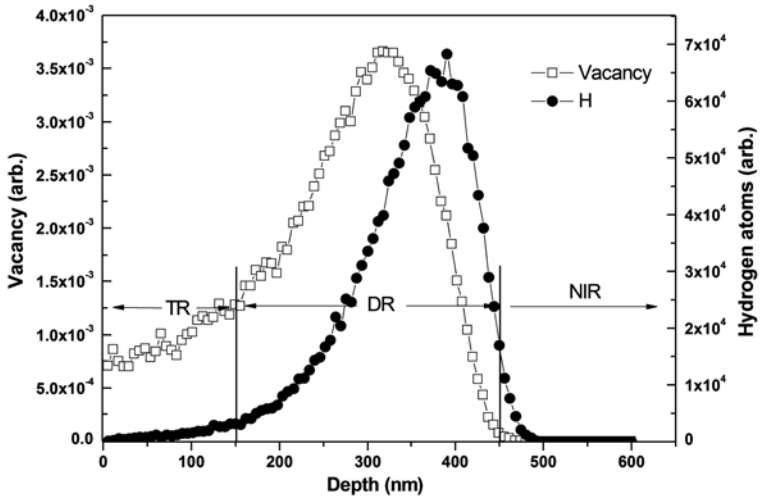

Fig. 1. SRIM calculation of damage profiles and ion distribution produced by 70 keV hydrogen ions. DR is the damage region. TR means the ion track region located between the surface and the DR, and NIR denotes the non-implanted region.

2.2 Hydrogen ion irradiation and annealing treatment

Already prepared polished sheet specimens were irradiated with hydrogen ions using an ion implanter in the Accelerator Laboratory of Wuhan University. The sample temperature was maintained at 400 °C ± 5 °C during irradiation, which was monitored by a thermocouple throughout the experiment process. Irradiations were performed using 70 keV H^+ to a fluence of 1×10^{16} ions m^{-2} and 1×10^{17} ions m^{-2}, corresponding to a maximum damage dose of 0.045 dpa and 0.45 dpa, respectively. The damage profiles and distributions of hydrogen ions calculated by SRIM 2008 [14] are shown in Fig. 1, where the displacement energy was 40 eV. Two specimens were irradiated to 0.045 dpa and 0.45 dpa, and corresponding irradiation times were 0.2 h and 2 h, respectively. In order to investigate the effect of elevated temperature, the third specimen was annealed at 400 °C for 2 h without

ion irradiation. The three specimens were then investigated by positron annihilation DB and CDB spectroscopy.

2.3 DB and CDB measurements

Positron annihilation DB and CDB measurements were carried out at the slow positron beam facility at the Institute of High Energy Physics, Beijing. Slow positrons were generated by a 1.85 GBq ^{22}Na radiation source. The positron beam energy range was 0.18 keV–20.18 keV. Importantly, the penetration depth of the incident positrons could cover the damage profiles and distribution of hydrogen ions. In the DB spectra, the *S* and *W* parameters were analyzed to characterize the defect information and the formation of Cu precipitates. The *S* parameter is defined as the ratio of the counts in central area of the 511 keV annihilation gamma ray peak (510.2 keV–511.8 keV) to the total counts of the whole peak (503.34 keV–518.66 keV). Annihilation γ-rays with a small energy displacement from the peak centre indicate positron annihilation with low-momentum valence electrons and thus the *S* parameter represents information on positron annihilation with vacancy-type defects. On the other hand, the *W* parameter is defined as the ratio of the counts at the outer regions of the peak (514.83 keV–518.66 keV and 503.34 keV–507.17 keV) to the total peak count. γ-rays with a large energy shift from the peak centre are due to positron annihilation with high-momentum regions of inner shell electrons and thus the *W* parameter conveys information on Cu element precipitates. In order to investigate the precipitation of Cu atoms further, two HPGe detectors were used to detect the 511 keV γ-ray pairs emitted by annihilation of positron and electron using the CDB technique, with a positron beam energy of 13.18 keV.

3. Results and discussion

According to the vacancies profiles in Fig. 1, the irradiated specimens were divided into three layers. The three layers have boundaries of about 0–150 nm, 150 nm–450 nm and the third layer is the bulk. In Fig. 1, DR is the damage region, where the incident ions produce a large number of defects. TR means the ion track region located between the surface and the DR. The third layer denotes the non-implanted region (NIR). The dependence of the *S* parameter on incident positron energy for Fe–0.3%Cu alloy annealed for 2 h and irradiated with different ion dose is shown in Fig. 2. The mean penetration depth of a slow positron is defined by the incident energy and is calculated by the empirical equation [15, 16].

$$Z(E) = \left(\frac{4 \times 10^4}{\rho}\right) E^{1.6} \tag{1}$$

where $Z(E)$ is the mean penetration depth below the surface and is expressed in nm, E is the incident energy (keV) of the slow positron and ρ is the density in units of kg m^{-3}. The calculated mean penetration depth below the surface of the slow positron beam is shown in the top x-axis of Fig. 2 according to Eq. (1).

The *S* parameter as a function of positron beam energy from 2 keV to 20 keV for the four samples (1. 400 °C 0.45 dpa, 2. 400 °C 0.045 dpa, 3. 400 °C 0 dpa and 4. as prepared) studied is shown in Fig. 2. The *S* parameter decreases with increasing positron energy for all samples. However, at all energies the *S* parameter for the 0.45 dpa sample is higher than that for the 0.045 dpa sample, indicating that higher irradiation dose produced more defects overall. In the DR, the values of the *S* parameter of the irradiated specimens were larger than that of the unirradiated ones from 13 keV to 20 keV, which clearly indicated that hydrogen ion irradiation produces a lot of vacancy-type defects in the DR. However, in contrast to the SRIM calculation (see Fig. 1), no peak in the *S* parameter formed in the irradiated specimens, and thus the experiment results are not consistent with the calculation. The reason may be that hydrogen atoms occupy the vacancy sites. This means that hydrogen atoms and vacancy-type defects combined and formed V-H complexes [15, 17]. Theoretical research showed

that implications of hydrogen could enhance vacancy activities and formation in α-Fe [18]. Because of the high diffusivity of hydrogen, the V-H complex may be destroyed and hydrogen atoms easily escape. Therefore, it is predicted that an annealing treatment could destroy the V-H complex and a peak in the *S* parameter would appear in the DR. Further research will focus on the effects of the annealing treatment in hydrogen ion-irradiated FeCu alloy. In the TR, the *S* parameter for unirradiated samples is larger than that for the irradiated ones from 2 keV to 8 keV. This is also an unexpected phenomenon. A reasonable interpretation would be that elevated temperature during irradiation leads to H atoms migrating to the surface and the formation of numerous V-H complexes due to occupation of defects by H. Thus, the formation of the V-H complexes leaded to a decrease of the *S* parameter in the TR of the irradiated specimens compared to the unirradiated specimens. However, another possibility which needs to be considered is the change of the positron diffusion length. In the range of 2 keV–8 keV, the *S* parameters of unirradiated specimens were higher than the intrinsic values due to the effect of the surface region. Thus, the positron diffusion length was reduced by irradiation-induced copper precipitates. As a result, the *S* parameter of the irradiated sample became close to the intrinsic value even in the same energy range. A third possibility may be the increase of the *W* parameter in irradiated specimens. The *W* parameter as a function of positron energy is plotted in Fig. 3. The *W* parameter of irradiated specimens was larger than that in unirradiated specimens because of the formation of copper precipitates. The ΔW parameter ($\Delta W = W_{\text{irradiated}} - W_{\text{unirradiated}}$) in the range 2 keV–8 keV was larger than that in the range 8 keV–20 keV. Therefore, the *S* parameter for irradiated samples became lower than that for the unirradiated ones from 2 keV to 8 keV.

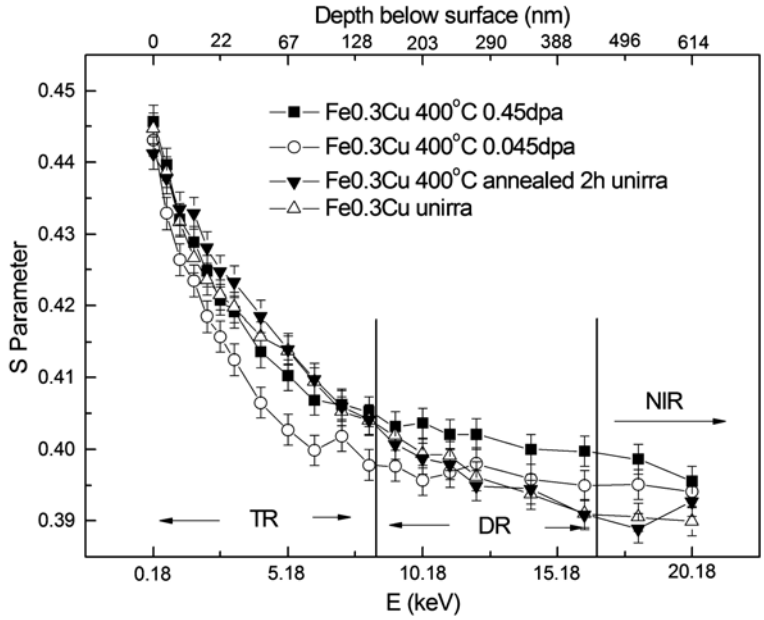

Fig. 2. *S–E* curves for Fe–0.3%Cu alloy annealed for 2 h and irradiated with different dose.

Figure 3 shows the *W* parameters of Fe–0.3%Cu alloy annealed for 2 h and irradiated with different dose. As stated above, the *W* parameter represents the positron annihilation with Cu 3d electrons and is defined as the ratio of the counts in high momentum ($18 \times 10^{-3} m_0 c < |P_L| < 30 \times 10^{-3} m_0 c$) regions in the DB spectrum to the total peak count, where m_0 is the electron rest mass, and c is the velocity of light. The irradiated specimens show an overall major increase in *W* parameter values compared to those of the unirradiated samples. In order to identify Cu precipitates further CDB was

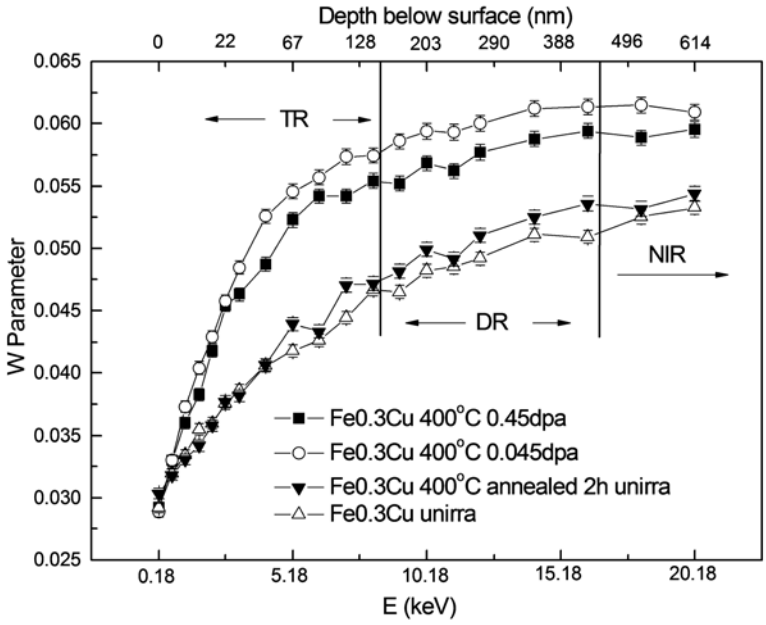

Fig. 3. *W–E* plots for the irradiated and unirradiated Fe–0.3%Cu samples. Positron annihilation with high-momentum core electron increase in irradiated specimens compared with the unirradiated specimen.

performed. Typical CDB spectra of the ratio of irradiated (0.045 dpa) Fe–0.3%Cu to unirradiated Fe–0.3%Cu annealed for 2 h plotted as a function of electron momentum is shown in Fig. 4. Previously, we have investigated the ratio curve of pure Cu that shows a peak at about $25 \times 10^{-3} m_0 c$ [5]. A broad peak appeared at the same position in the case of irradiated Fe–0.3%Cu alloy, and it came from Cu precipitates [2, 19]. Therefore, this illustrates that the precipitation of Cu atoms formed easily at low irradiation dose. In addition, there is no obvious distinction in the *W* parameter values between the unirradiated specimen and the annealed Fe–0.3%Cu alloy in Fig. 3. This means that no obvious Cu precipitates formed when Fe–0.3%Cu alloy was annealed for 2 h at 400 °C. Barbu *et al*. showed that the mechanism of Cu precipitation was identical in FeCu alloy under thermal aging at 500 °C and electron irradiation at 290 °C [3, 20]. Single elevated temperature (400 °C) thermal treatment does not lead to obvious Cu atom precipitates in the present work.

We now attempt to propose an explanation for the Cu precipitation behavior in irradiated FeCu alloy that we found in this study. Figure 5 shows a *S–W* plot for all samples studied and shows the correlation between Cu precipitation formation and irradiation induced defects (vacancy-type defects and V-H complexes). Lines 1 to 3 correspond to an irradiation dose of 0, 0.045 dpa and 0.45 dpa, respectively. Line 4 corresponds to the specimen annealed for 2 h at 400 °C. The *S–W* plots follow a near linear relation from the surface region to bulk region for all samples. However, the slope of the plot changes clearly in the irradiated alloys compared to the unirradiated samples. The slopes of the irradiated specimens were larger than that of the unirradiated samples indicating that the mechanism of positron annihilation was changed in hydrogen ion irradiated specimens. According to the results shown in Fig. 2, the *S* parameter increased with an increasing irradiation dose from 0.045 dpa to 0.45 dpa in the DR indicating a larger number of vacancy-type defects and V-H complexes were formed. However, since Cu atoms are easily aggregated by vacancy migration [2], it is likely that the nucleation of small Cu precipitates occurs prior to the formation of V-H complexes. The V-H complex in an irradiation induced defect and could be regarded as a sink, which could absorb more small Cu precipitates. The aggregation of Cu atoms grew and coarsened finally with increasing irradiation dose.

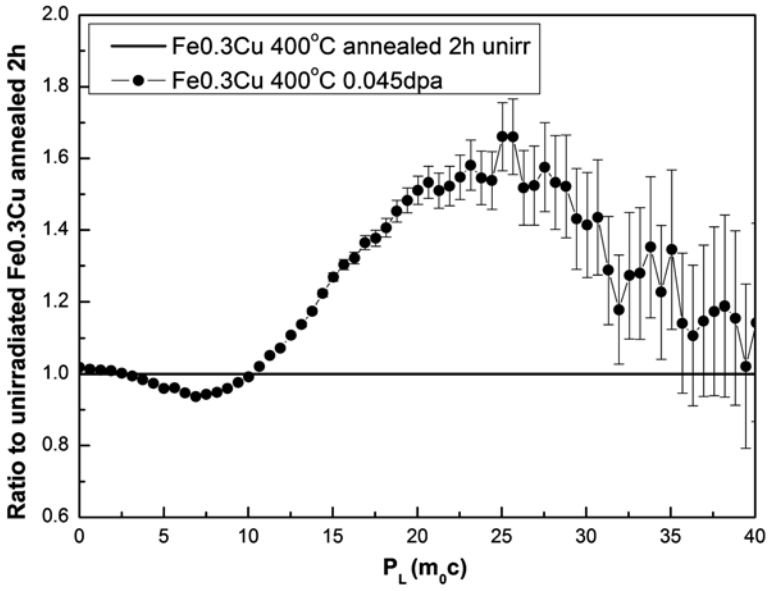

Fig. 4. Typical CDB ratio spectra of irradiated Fe–0.3%Cu to unirradiated Fe–0.3%Cu annealed for 2 h.

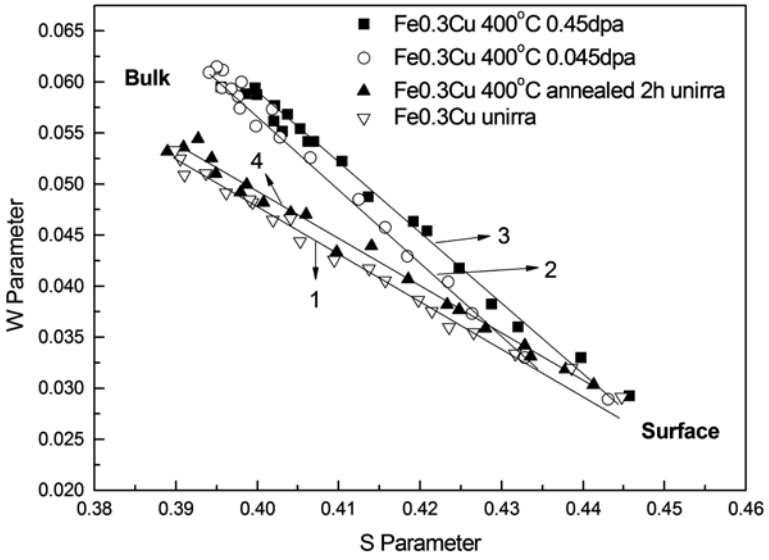

Fig. 5. *S*–*W* curves for the Fe–Cu alloys studied. The lines labeled 1 to 3 correspond to an irradiation dose of 0 dpa, 0.045 dpa and 0.45 dpa, respectively. Line 4 corresponds to the specimen annealed for 2 h at 400 °C. The experimental data follows a linear relation from the surface to bulk, but the slopes for the irradiated specimens (lines 2 and 3) were different from the unirradiated specimens (lines 1 and 4).

4. Conclusion

This work examined the formation of V-H complexes and Cu precipitates in Fe–0.3%Cu binary model alloys after hydrogen ion irradiation and annealing treatment at 400 °C via DB and CDB. In the irradiated specimens, hydrogen atoms occupied vacancy sites and V-H complexes were formed. An

analysis of the *W* parameter and CDB results indicated that Cu precipitates formed easily under lower irradiation dose at elevated temperature. It is likely that the nucleation of small Cu precipitates occurs prior to the formation of V-H complexes, and V-H complexes could absorb more small Cu precipitates as sinks.

Acknowledgment

This work is supported by the National Natural Science Foundation of China (91026006 and 91226103) and the Xie Jialin Foundation of IHEP.

References

[1] Y. Nishiyama, K. Onizawa, M. Suzuki, J. W. Anderegg, Y. Nagai, T. Toyama, M. Hasegawa, and J. Kameda: Acta Mater. **56** (2008) 4510.
[2] Q. Xu, T. Yoshiie, and K. Sato: Phys. Rev. B **73** (2006) 134115.
[3] M. H. Mathon, A. Barbu, F. Dunstetter, F. Maury, N. Lorenzelli, and C. H. de Novion: J. Nucl. Mater. **245** (1997) 224.
[4] Q. Xu and T. Yoshiie: Philos. Mag. **91** (2011) 3716.
[5] X. Z. Cao, P. Zhang, Q. Xu, K. Sato, H. Tsuchida, G. D. Cheng, H. B. Wu, X. P. Jiang, R. S. Yu, B. Y. Wang, and L. Wei: J. Phys. Conf. Ser. **443** (2013) 012017.
[6] G. R. Odette and G. E. Lucas: Radiat. Eff. Defects Solids **144** (1998) 189.
[7] W. J. Phythian, and C. A. English: J. Nucl. Mater. **205** (1993) 162.
[8] K. Fukuya, K. Ohno, H. Nakata, S. Dumbill, and J. M. Hyde: J. Nucl. Mater. **312** (2003) 163.
[9] R. G. Carter, N. Soneda, K. Dohi, J. M. Hyde, C. A. English, and W. L. Server: J. Nucl. Mater. **298** (2001) 211.
[10] T. Yoshiie, Q. Xu, and K. Sato: Nucl. Instrum. Methods Phys. Res. Sect. B-Beam Interact. Mater. Atoms **303** (2013) 37.
[11] Y. Nagai, Z. Tang, M. Hasegawa, T. Kanai, and M. Saneyasu: Phys. Rev. B **63** (2001) 134110.
[12] F. Hori, S. Tanaka, E. Kuramoto, and A. Iwase: Nucl. Instrum. Methods Phys. Res. Sect. B-Beam Interact. Mater. Atoms **245** (2006) 180.
[13] G. S. Was, J. T. Busby, T. Allen, E. A. Kenik, A. Jenssen, S. M. Bruemmer, J. Gan, A. D. Edwards, P. M. Scott, and P. L. Andreson: J. Nucl. Mater. **300** (2002) 198.
[14] http://www.srim.org/.
[15] J. Qiu, Y. Xin, X. Ju, L. P. Guo, B. Y. Wang, Y. R. Zhong, Q. Y. Huang, and Y. C. Wu: Nucl. Instrum. Methods Phys. Res. Sect. B-Beam Interact. Mater. Atoms **267** (2009) 3162.
[16] R. S. Wang, X. B. Liu, A. Ren, J. Jiang, C. L. Xu, P. Huang, Y. C. Wu, C. H. Zhang, and X. T. Wang: Nucl. Instrum. Methods Phys. Res. Sect. B-Beam Interact. Mater. Atoms **307** (2013) 545.
[17] J. Qiu, X. Ju, Y. Xin, S. Liu, and B. Y. Wang: J. Nucl. Mater. **411** (2011) 20.
[18] Y. Tateyama and T. Ohno: Phys. Rev. B **67** (2003) 174105.
[19] Z. Tang, M. Hasegawa, Y. Nagai, and M. Saito: Phys. Rev. B **65** (2002) 195108.
[20] A. Barbu, M. H. Mathon, F. Maury, J. F. Belliard, B. Beuneu, and C. H. de Novion: J. Nucl. Mater. **257** (1998) 206.